Primitive quantum gates for an $SU(2)$ discrete subgroup: Binary octahedral

Erik J. Gustafson,[1,2,3,4] Henry Lamm,[1,2,*] and Felicity Lovelace[5,†]

[1]Superconducting and Quantum Materials System Center (SQMS), Batavia, Illinois 60510, USA
[2]Fermi National Accelerator Laboratory, Batavia, Illinois 60510, USA
[3]Quantum Artificial Intelligence Laboratory (QuAIL),
NASA Ames Research Center, Moffett Field, California 94035, USA
[4]USRA Research Institute for Advanced Computer Science (RIACS), Mountain View, California 94043, USA
[5]Department of Physics, University of Illinois at Chicago, Chicago, Illinois 60607, USA

(Received 2 January 2024; accepted 13 February 2024; published 13 March 2024)

We construct a primitive gate set for the digital quantum simulation of the 48-element binary octahedral ($\mathbb{BO}$) group. This non-Abelian discrete group better approximates $SU(2)$ lattice gauge theory than previous work on the binary tetrahedral group at the cost of one additional qubit—for a total of six—per gauge link. The necessary primitives are the inversion gate, the group multiplication gate, the trace gate, and the $\mathbb{BO}$ Fourier transform.

DOI: 10.1103/PhysRevD.109.054503

I. INTRODUCTION

The possibilities for quantum utility in lattice gauge theories (LGT) are legion [1–4]. Perhaps foremost, it provides an elegant solution to the sign problem which results in exponential scaling of classical computing resources [5] which precludes large-scale simulations of dynamics, at finite fermion density, and in the presence of topological terms. In order to study these fundamental physics topics, a number of quantum subroutines are required.

The first task is preparing strongly-coupled states of interest including ground states [6–12], thermal states [13–23], and colliding particles [24–34]. For applications to dynamics, the time-evolution operator $U(t) = e^{-iHt}$ must be approximated and many different choices exist; Trotterization [35,36], random compilation [37,38], Taylor series [39], qubitization [40], quantum walks [41], signal processing [42], linear combination of unitaries [38,43], and variational approaches [44–47], each with their own trade-offs. Important alongside state preparation and evolution is the need to develop efficient techniques [48–51] and formulations [52–63] for measuring physical observables. Necessary for acheiving this, one may further use algorithmic improvements such as error mitigation and correction [64–79], improved Hamiltonians [80,81] and quantum smearing [82] to reduce errors from quantum noise and theoretical approximations. Beyond direct simulations, quantum computers could also accelerate classical lattice gauge theory simulations by reducing autocorrelation [83–86] and optimizing interpolating operators [87,88].

Across this cornucopia, there exist a set of fundamental group theoretic operations that LGT requires [52]. Via this identification of primitive subroutines, the problem of formulating quantum algorithms for LGT can be divided into deriving said group-dependent primitives [89–91] and group-independent algorithmic design [80,82,91,92].

With this notion in mind, one can turn to digitizing the infinite-dimensional Hilbert space of the gauge bosons. Many proposals exist that prioritizing theoretical and algorithmic facets of the problem differently [93–133]. For some digitized theories, there may be no nontrivial continuum limit [122,123,125,134–141]. Furthermore, the efficacy of a gauge digitization can be dimension dependent [89,90,117,142]. While all digitizations consider the relative quantum memory costs, the consequences of digitization on gate costs are more limited. Despite this, recent work has made abundantly clear that the number of expensive fixed-point arithmetic required can vary by orders of magnitude [36,143].

One promising digitization that uses comparatively few qubits and avoids fixed-point arithmetic is the discrete subgroup approximation [66,101,103–107,128,144,145]. This method was explored in the 1970s and 1980s to reduce memory and runtime of Euclidean LGT on classical computers. The replacement of $U(1)$ by $\mathbb{Z}_N$ was considered first [146,147] and eventually extended to the crystal-like subgroups of $SU(N)$ [103,104,128,148–153]. Some studies

*hlamm@fnal.gov
†fl16@uic.edu

were even performed with dynamical fermions [154,155]. Theoretical work has established that the discrete subgroup approximation corresponds to continuous groups broken by a Higgs mechanism [156–160].

LGT calculations are performed at fixed lattice spacing $a = a(\beta)$ which for asymptotically free theories approach zero as $\beta \to \infty$. Finite a leads to discrepancies from the continuum results, but provided one simulates in the *scaling regime* below $a_s(\beta_s)$, these errors are well-behaved. On the lattice, the breakdown of the discrete subgroup approximation manifests as a *freeze-out* a_f (or coupling β_f) where the gauge links become "frozen" to the identity. Despite this, the approximation error for Euclidean calculations can be tolerable provided $a_s \gtrsim a_f$ $(\beta_s \lesssim \beta_f)$ [104,152]. Further, a connection between the couplings and lattice spacings of Minkowski and Euclidean lattice field theories has been shown [144,153,161], which suggests similarly controllable digitization error on large-scale quantum simulations and a way for determining viable approximations.

The freezing transitions are known in $3+1d$ when the Wilson action is used. Given the known connection between the Wilson action and the Kogut-Susskind Hamiltonian H_{KS} [162], this provides insight into the viable groups for quantum simuations. Approximating $U(1)$ by $\mathbb{Z}_{n\geq 5}$ satisfies $\beta_f > \beta_s$, with $\beta_f \propto 1 - \cos^{-1}(2\pi/n)$. In the case of non-Abelian gauge groups, there are limited number of crystal-like subgroups. $SU(2)$, with $\beta_s = 2.2$ has three; the 24-element binary tetrahedral $\mathbb{BT}$ $(\beta_f = 2.24(8))$, the 48-element binary octahedral $\mathbb{BO}$ $(\beta_f = 3.26(8))$, and the 120-element binary icosahedral $\mathbb{BI}$ $(\beta_f = 5.82(8))$ [104]. Thus, while $\mathbb{BT}$ require only 5 qubits, due to its low β_f it is unlikely H_{KS} can be used for quantum simulation but a modified or improved Hamiltonians H_I [80,81] could prove sufficient [104,128,151,152]. The effects on the scaling regime when including fermions is a more subtle question. The structure of discrete groups makes it difficult to leverage traditional Monte Carlo schemes to investigate the transition such as shown in Fig. 1. Qualitiatively one could make the following insights; for sufficiently heavy fermions one would expect the scaling behavior to be slightly increased, while the effects for lighter fermions could drastically change the scaling regime in β due to the lower cost of pair creation.

In this work, we consider the smallest crystal-like subgroup of a $SU(2)$ with $a_f > a_s$—$\mathbb{BO}$ which requires 6 qubits per register. A number of smaller non-Abelian groups have been considered previously. Quantum simulations of the $2N$-element dihedral groups, D_N, while not crystal-like, have been extensively studied [52,89,101,163]. The 8-element $\mathbb{Q}_8$ subgroup of $SU(2)$ has also been investigated [145]. In [90], quantum circuits for $\mathbb{BT}$ were constructed and resource estimates were obtained using the H_I of [80].

In the interest of studying near-term quantum simulations, we should consider $2+1d$ theories in addition to $3+1d$ ones. Using classical lattice simulations, we determined $\beta_f > \beta_s$ in both space-times for the Wilson action (See Fig. 1). Thus quantum simulations with $\mathbb{BO}$ can be performed with the Kogut-Susskind Hamiltonian [164], although using an improved Hamiltonian can reduce either qubits or lattice spacing errors [80].

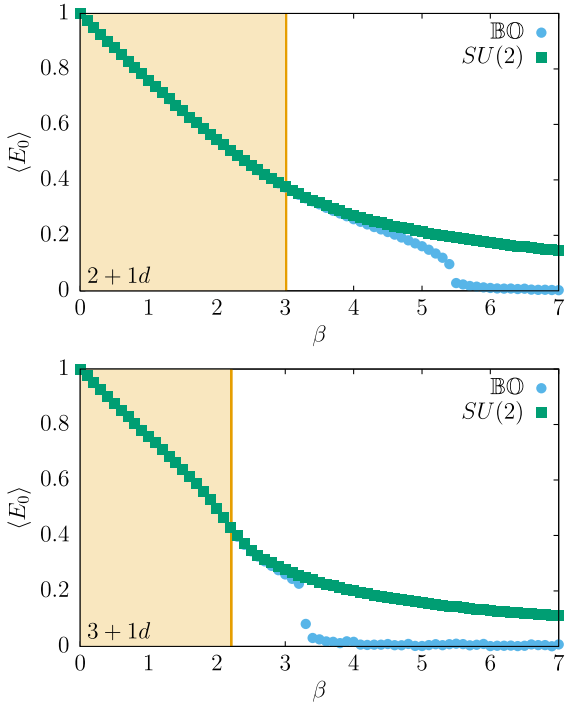

FIG. 1. Euclidean calculations of lattice energy density $\langle E_0 \rangle$ of $\mathbb{BO}$ as measured by the expectation value of the plaquette as a function of Wilson coupling β on 8^d lattices for (top) $2+1d$ (bottom) $3+1d$. The shaded region indicates $\beta \leq \beta_s$.

In this paper, the four necessary primitive quantum gates (inversion, multiplication, trace, and Fourier) for quantum simulation of $\mathbb{BO}$ theories on qubit-based computers are constructed. In Sec. II, important group theory for $\mathbb{BO}$ is summarized and the qubit encoding is presented. A brief review of entangling gates used is found in Sec. III. Section IV provides an overview of the primitive gates. This is followed by explicit quantum circuits for each gate for $\mathbb{BO}$; the inversion gate in Sec. V, the multiplication gate in Sec. VI, the trace gate in Sec. VII, and the Fourier transform gate in Sec. VIII. Using these gates, Sec. IX presents a resource estimates for simulating $3+1d$ $SU(2)$. We conclude and discuss future work in Sec. X.

II. PROPERTIES OF $\mathbb{BO}$

The simulation of LGT requires defining a register where one can store the state of a bosonic link variable which we call a $G-$register. To construct the $\mathbb{BO}$-register in term of integers, it is necessary to map the 48 elements of $\mathbb{BO}$ to the integers [0, 47]. A clean way to obtain this is to write every element of $\mathbb{BO}$ as an ordered product of five generators with

exponents written in terms of the binary variables x_i with $i = [1, 6]$:

$$g = (-1)^{x_1}\mathbf{j}^{x_2}\mathbf{k}^{x_3}\mathbf{u}^{2x_4+x_5}\mathbf{t}^{x_6}, \tag{1}$$

with

$$\mathbf{u} = -\frac{1}{2}(\mathbb{1} + \mathbf{i} + \mathbf{j} + \mathbf{k}) \quad \text{and} \quad \mathbf{t} = \frac{1}{\sqrt{2}}(\mathbb{1} + \mathbf{i}) \tag{2}$$

and $\mathbf{i}$, $\mathbf{j}$, $\mathbf{k}$ are the unit quaternions which in the 2d irreducible representation (irrep) correspond to Pauli matrices. With the construction of Eq. (1), the $\mathbb{BO}$-register is given by a binary qubit encoding with the ordering $|x_6x_5x_4x_3x_2x_1\rangle$. While there exist 2^6 possible state in a 6 qubit register, we only consider the 48 states where $x_4 + x_5 \leq 1$ represent the group elements. The states where $x_4 = x_5 = 1$ correspond to *forbidden states*. In this work we will use a short hand $|N\rangle$ where N is the decimal representation of the binary $x_6x_5x_4x_3x_2x_1$. For example,

$$\frac{1}{\sqrt{2}}\begin{pmatrix} -i & -1 \\ 1 & i \end{pmatrix} = (-1)^1\mathbf{j}^0\mathbf{k}^1\mathbf{u}^{2\times 0+0}\mathbf{t}^1 \to |100101\rangle = |37\rangle. \tag{3}$$

The $\mathbf{i}$, $\mathbf{j}$, and $\mathbf{k}$ generators anticommute with each other. Additional useful relations are

$$\begin{aligned} &\mathbf{i}^2 = \mathbf{j}^2 = \mathbf{k}^2 = -\mathbb{1}, \qquad \mathbf{u}^3 = \mathbb{1}, \qquad \mathbf{t}^2 = \mathbf{i}, \\ &\mathbf{ij} = \mathbf{k}, \qquad \mathbf{jk} = \mathbf{i}, \qquad \mathbf{ki} = \mathbf{j}, \\ &\mathbf{iu} = \mathbf{uk}, \qquad \mathbf{ju} = \mathbf{ui}, \qquad \mathbf{ku} = \mathbf{uj}, \\ &\mathbf{it} = \mathbf{ti}, \qquad -\mathbf{jt} = \mathbf{tk}, \qquad \mathbf{kt} = \mathbf{tj}, \end{aligned} \tag{4}$$

The character table (Table I) lists important group properties; the different irreps, denoted as ρ_i,can be identified by the value of their character,which correspond to the columns in Table I, acting on each element. The final row indicates the binary state corresponding to group elements in a given character. An irrep's dimension is the value of the character of 1. There are three $1d$ irreps, three $2d$ irreps (one real and two complex), and one $3d$ irrep. To derive the Fourier transform, it is necessary to know a matrix presentation of each irrep. Based on our qubit mapping, given a presentation of -1, $\mathbf{i}$, $\mathbf{j}$, and $\mathbf{l}$ we can construct any element of the group from Eq. (1). With the nth root of unity $\omega_n = e^{2\pi i/n}$, the matrix presentations of our generators in each irrep are found in Table II.

III. QUBIT GATES

To construct our primitive gates, we chose a universal, albeit redundant, basic qubit quantum gate set. We use the

TABLE I. Character table of $\mathbb{BO}$ from [165] and an enumeration of the elements in the given class.

Size	1	1	12	6	8	8	6	6
Order	1	2	4	4	6	3	8	8
ρ_1	1	1	1	1	1	1	1	1
ρ_2	1	1	−1	1	1	1	−1	−1
ρ_3	2	2	0	2	−1	−1	0	0
ρ_4	2	−2	0	0	1	−1	$\sqrt{2}$	$-\sqrt{2}$
ρ_5	2	−2	0	0	1	−1	$-\sqrt{2}$	$\sqrt{2}$
ρ_6	3	3	−1	−1	0	0	1	1
ρ_7	3	3	1	−1	0	0	−1	−1
ρ_8	4	−4	0	0	−1	1	0	0
$\|g\rangle$	$\|0\rangle$	$\|1\rangle$	$\|34\rangle - \|37\rangle$	$\|2\rangle - \|7\rangle$	$\|9\rangle$, $\|11\rangle$	$\|8\rangle$, $\|10\rangle$	$\|32\rangle$, $\|39\rangle$	$\|33\rangle$, $\|38\rangle$
			$\|44\rangle - \|49\rangle$		$\|13\rangle$, $\|15\rangle$	$\|12\rangle$, $\|14\rangle$	$\|41\rangle$, $\|43\rangle$	$\|40\rangle$, $\|42\rangle$
			$\|52\rangle$, $\|53\rangle$		$\|17\rangle$, $\|18\rangle$	$\|16\rangle$, $\|19\rangle$	$\|50\rangle$, $\|54\rangle$	$\|51\rangle$, $\|55\rangle$
					$\|20\rangle$, $\|22\rangle$	$\|21\rangle$, $\|23\rangle$		

Pauli gates $p = X$, Y, Z and their arbitrary rotation generalizations $R_p(\theta) = e^{i\theta p/2}$. When decomposing onto fault-tolerant devices, how these are decomposed in terms of the $T = \mathrm{diag}(1, e^{i\pi/4})$ gate becomes relevant to resource estimations.

We also use the SWAP gate

$$\mathrm{SWAP}|a\rangle \otimes |b\rangle = |b\rangle \otimes |a\rangle,$$

and CNOT gate

$$\mathrm{CNOT}|a\rangle \otimes |b\rangle = |a\rangle \otimes |b \oplus a\rangle.$$

We further use the multiqubit C^{n}NOT—of which C^{2}NOT is called the Toffoli gate—and CSWAP (Fredkin) gates. The C^{n}NOT gate consists of one target qubit and n control qubits. For example, the Toffoli in terms of modular arithmetic is

$$\mathrm{C^2NOT}|a\rangle \otimes |b\rangle \otimes |c\rangle = |a\rangle \otimes |b\rangle \otimes |c \oplus ab\rangle.$$

The CSWAP gate swaps two qubit states if the control is in the $|1\rangle$ state:

$$\begin{aligned} \mathrm{CSWAP}|a\rangle \otimes |b\rangle \otimes |c\rangle = |a\rangle \otimes |b(1 \oplus a) \oplus ac\rangle \\ \otimes |c(1 \oplus a) \oplus ab\rangle. \end{aligned}$$

IV. OVERVIEW OF PRIMITIVE GATES

One can define any quantum circuit for gauge theories via a set of primitive gates, of which one choice is inversion $\mathfrak{U}_{-1}$, multiplication $\mathfrak{U}_\times$, trace $\mathfrak{U}_{\mathrm{Tr}}$, and Fourier transform $\mathfrak{U}_F$ [52]. The inversion gate, $\mathfrak{U}_{-1}$, takes a G-register to its inverse:

TABLE II. Matrix representations of the generators used for digitization of $\mathbb{BO}$.

g	-1	**j**	**k**	**u**	**t**
ρ_1	1	1	1	1	1
ρ_2	1	1	1	1	-1
ρ_3	$\begin{pmatrix} 1 & 0 \\ 0 & 1 \end{pmatrix}$	$\begin{pmatrix} 1 & 0 \\ 0 & 1 \end{pmatrix}$	$\begin{pmatrix} 1 & 0 \\ 0 & 1 \end{pmatrix}$	$\begin{pmatrix} \omega_3^2 & 0 \\ 0 & \omega_3 \end{pmatrix}$	$\begin{pmatrix} 0 & 1 \\ 1 & 0 \end{pmatrix}$
ρ_4	$\begin{pmatrix} -1 & 0 \\ 0 & -1 \end{pmatrix}$	$\begin{pmatrix} 0 & 1 \\ -1 & 0 \end{pmatrix}$	$\begin{pmatrix} i & 0 \\ 0 & -i \end{pmatrix}$	$\frac{1}{2}\begin{pmatrix} -1-i & -1+i \\ 1+i & -1+i \end{pmatrix}$	$\frac{1}{\sqrt{2}}\begin{pmatrix} 1 & -i \\ -i & 1 \end{pmatrix}$
ρ_5	$\begin{pmatrix} -1 & 0 \\ 0 & -1 \end{pmatrix}$	$\begin{pmatrix} 0 & 1 \\ -1 & 0 \end{pmatrix}$	$\begin{pmatrix} i & 0 \\ 0 & -i \end{pmatrix}$	$\frac{1}{2}\begin{pmatrix} -1-i & -1+i \\ 1+i & -1+i \end{pmatrix}$	$\frac{1}{\sqrt{2}}\begin{pmatrix} -1 & i \\ i & -1 \end{pmatrix}$
ρ_6	$\begin{pmatrix} 1 & 0 & 0 \\ 0 & 1 & 0 \\ 0 & 0 & 1 \end{pmatrix}$	$\begin{pmatrix} -1 & 0 & 0 \\ 0 & 1 & 0 \\ 0 & 0 & -1 \end{pmatrix}$	$\begin{pmatrix} 1 & 0 & 0 \\ 0 & -1 & 0 \\ 0 & 0 & -1 \end{pmatrix}$	$\begin{pmatrix} 0 & 1 & 0 \\ 0 & 0 & 1 \\ 1 & 0 & 0 \end{pmatrix}$	$\begin{pmatrix} 0 & -1 & 0 \\ 1 & 0 & 0 \\ 0 & 0 & -1 \end{pmatrix}$
ρ_7	$\begin{pmatrix} 1 & 0 & 0 \\ 0 & 1 & 0 \\ 0 & 0 & 1 \end{pmatrix}$	$\begin{pmatrix} -1 & 0 & 0 \\ 0 & 1 & 0 \\ 0 & 0 & -1 \end{pmatrix}$	$\begin{pmatrix} 1 & 0 & 0 \\ 0 & -1 & 0 \\ 0 & 0 & -1 \end{pmatrix}$	$\begin{pmatrix} 0 & 1 & 0 \\ 0 & 0 & 1 \\ 1 & 0 & 0 \end{pmatrix}$	$\begin{pmatrix} 0 & 1 & 0 \\ -1 & 0 & 0 \\ 0 & 0 & 1 \end{pmatrix}$
ρ_8	$\begin{pmatrix} -1 & 0 & 0 & 0 \\ 0 & -1 & 0 & 0 \\ 0 & 0 & -1 & 0 \\ 0 & 0 & 0 & -1 \end{pmatrix}$	$\begin{pmatrix} 0 & -i & 0 & 0 \\ -i & 0 & 0 & 0 \\ 0 & 0 & -i & 0 \\ 0 & 0 & 0 & i \end{pmatrix}$	$\begin{pmatrix} i & 0 & 0 & 0 \\ 0 & -i & 0 & 0 \\ 0 & 0 & 0 & -i \\ 0 & 0 & -i & 0 \end{pmatrix}$	$\frac{\omega_3}{2}\begin{pmatrix} (-1-i)\omega_3 & (1+i)\omega_3 & 0 & 0 \\ (-1+i)\omega_3 & (-1+i)\omega_3 & 0 & 0 \\ 0 & 0 & -1+i & 1+i \\ 0 & 0 & -1+i & -1-i \end{pmatrix}$	$\begin{pmatrix} 0 & 0 & 0 & -1 \\ 0 & 0 & 1 & 0 \\ 1 & 0 & 0 & 0 \\ 0 & 1 & 0 & 0 \end{pmatrix}$

$$\mathfrak{U}_{-1}|g\rangle = |g^{-1}\rangle. \tag{5}$$

$\mathfrak{U}_\times$ takes a target G-register and changes it to the left product controlled by a second G-register:

$$\mathfrak{U}_\times|g\rangle|h\rangle = |g\rangle|gh\rangle. \tag{6}$$

Left multiplication is sufficient for a minimal set as right multiplication can be obtained from two applications of $\mathfrak{U}_{-1}$ and $\mathfrak{U}_\times$, albeit resource costs can be further reduced by an explicit construction [80].

Traces of group elements generally define the lattice Hamiltonian. We can implement the evolution with respect to these terms via:

$$\mathfrak{U}_{\mathrm{Tr}}(\theta)|g\rangle = e^{i\theta \mathrm{Re}\,\mathrm{Tr}\,g}|g\rangle. \tag{7}$$

The final gate of this set is $\mathfrak{U}_F$. The Fourier transform, $\hat{f}$, of a function f over a finite G is

$$\hat{f}(\rho) = \sum_{g\in G}\sqrt{\frac{d_\rho}{|G|}}f(g)\rho(g), \tag{8}$$

where $|G|$ is the size of the group, d_ρ is the dimensionality of the irrep ρ. The inverse transform is given by

$$f(g) = \sum_{\rho\in\hat{G}}\sqrt{\frac{d_\rho}{|G|}}\mathrm{Tr}(\hat{f}(\rho)\rho(g^{-1})), \tag{9}$$

where the dual $\hat{G}$ is the set of irrep of G. A paradigm of this unitary matrix is shown in Fig. 2 which can then be transformed into a gate. $\mathfrak{U}_F$ then acts on a single G-register with some amplitudes $f(g)$ which rotate it into the irrep basis:

$$\mathfrak{U}_F\sum_{g\in G}f(g)|g\rangle = \sum_{\rho\in\hat{G}}\hat{f}(\rho)_{ij}|\rho,i,j\rangle. \tag{10}$$

V. INVERSION GATE

Consider a $\mathbb{BO}$-register storing the group element given by $g = (-1)^{x_1}\mathbf{j}^{x_2}\mathbf{k}^{x_3}\mathbf{u}^{2x_4+x_5}\mathbf{t}^{x_6}$. The effect of the inversion gate on this register is to transform it to

$$|g\rangle = |x_1x_2x_3x_4x_5x_6\rangle \to |g^{-1}\rangle = |y_1y_2y_3y_4y_5y_6\rangle. \tag{11}$$

Where y_i must be determined. With Eq. (1), g^{-1} is

$$g^{-1} = \mathbf{t}^{8-x_6}\mathbf{u}^{3-(2x_4+x_5)}\mathbf{k}^{x_3}\mathbf{j}^{x_2}(-1)^{x_1+x_2+x_3}. \quad (12)$$

A systematic way to build the $\mathfrak{U}_{-1}$ of $\mathbb{BO}$ is to embed the inverse gates of subgroups of $\mathbb{BO}$. We start with the expression of Eq. (12), and begin by reordering the $\mathbb{Q}_8$ subgroup so that the element is of the form:

$$\mathbf{k}^{x_3}\mathbf{j}^{x_2}(-1)^{x_1+x_2+x_3} = (-1)^{a_1}\mathbf{j}^{a_2}\mathbf{k}^{a_3}, \quad (13)$$

where $a_1 = x_1 + x_2 + x_3 + x_2x_3$ and $a_2 = x_2$, $a_3 = x_3$. The next step is commuting through $\mathbf{u}$ to obtain

$$\mathbf{u}^{3-(2x_4+x_5)}(-1)^{a_1}\mathbf{j}^{a_2}\mathbf{k}^{a_3} = (-1)^{b_1}\mathbf{j}^{b_2}\mathbf{k}^{b_3}\mathbf{u}^{2b_4+b_5}, \quad (14)$$

which corresponds to the $\mathbb{BT}$ inverse gate where

$$\begin{aligned} b_2 &= a_2(1+x_4) + a_3(x_4+x_5),\\ b_3 &= a_3(1+x_5) + a_2(x_4+x_5),\\ b_4 &= x_5,\\ b_5 &= x_4, \end{aligned} \quad (15)$$

while $b_1 = a_1$ is unchanged. Finally, commuting through $\mathbf{t}$,

$$\mathbf{t}^{8-x_6}(-1)^{b_1}\mathbf{j}^{b_2}\mathbf{k}^{b_3}\mathbf{u}^{2b_4+b_5} = (-1)^{y_1}\mathbf{j}^{y_2}\mathbf{k}^{y_3}\mathbf{u}^{2y_4+y_5}\mathbf{t}^{y_6}. \quad (16)$$

Propagating $\mathbf{t}^{x_6}$ through the $\mathbb{Q}_8$ portion yields $g^{-1} = (-1)^{c_1}\mathbf{j}^{c_2}\mathbf{k}^{c_3}\mathbf{t}^{x_6}\mathbf{u}^{2b_4+b_5}$, where

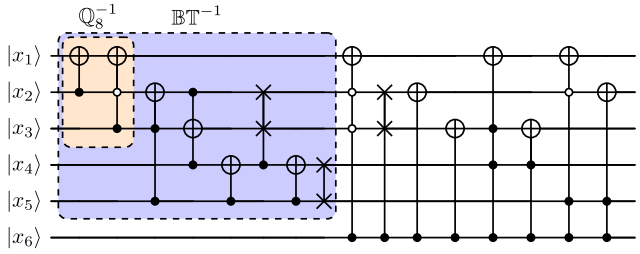

FIG. 3. Quantum circuit for $\mathfrak{U}_{-1}$ for $\mathbb{BO}$. The subgates correspond to $\mathfrak{U}_{-1}$ for $\mathbb{Q}_8$ ($\mathbb{BT}$) in orange (blue).

$$\begin{aligned} c_1 &= b_1 + x_6(1-b_3)(1-b_2),\\ c_2 &= (1-b_3)x_6 + (1-x_6)b_2,\\ c_3 &= (1-b_2)x_6 + (1-x_6)b_3. \end{aligned}$$

Finally, propagating through $\mathbf{t}^{x_6}$ through $\mathbf{u}^{2b_4+b_5}$ yields,

$$\begin{aligned} y_1 &= c_1 + x_6(b_4(1-c_2) + c_3b_5),\\ y_2 &= c_2 + b_4x_6,\\ y_3 &= c_3 + (b_4+b_5)x_6,\\ y_4 &= x_6b_5 + (1-x_6)b_4,\\ y_5 &= x_6b_4 + (1-x_6)b_5, \end{aligned} \quad (17)$$

with $y_6 = x_6$. Together, this yields for $|g\rangle$ to $|g^{-1}\rangle$:

$$\begin{aligned} y_1 &= x_1 + x_2x_3x_6 + x_2x_3 + x_2x_5x_6 + x_2x_6 + x_2 + x_3x_4x_6 + x_3x_6 + x_3 + x_4x_6 + x_6,\\ y_2 &= x_2x_4 + x_2x_5x_6 + x_2x_6 + x_2 + x_3x_4x_6 + x_3x_4 + x_3x_5 + x_3x_6 + x_5x_6 + x_6,\\ y_3 &= (x_2+x_3)(x_5+x_6) + x_6(x_4(x_3+1) + x_5(x_2+1)) + x_2x_4 + x_3 + x_6,\\ y_4 &= (x_4+x_5)x_6 + x_5,\\ y_5 &= (x_4+x_5)x_6 + x_4, \end{aligned} \quad (18)$$

where $y_6 = x_6$ is unaffected. We provide the quantum circuit for this gate in Fig. 3.

VI. MULTIPLICATION GATE

Given two $\mathbb{BO}$-registers $|g\rangle = |\prod x_i\rangle$ and $|h\rangle = |\prod y_i\rangle$, we want $|gh\rangle = |\prod z_i\rangle$. Here, we again decompose

$$\mathfrak{U}_\times = \mathfrak{U}_{\times,-1}\mathfrak{U}_{\times,\mathbf{j}}\mathfrak{U}_{\times,\mathbf{k}}\mathfrak{U}_{\times,\mathbf{u}_2}\mathfrak{U}_{\times,\mathbf{u}_1}\mathfrak{U}_{\times,\mathbf{t}} \quad (19)$$

into gates controlled by a single qubits. For each step, we use temporary variables indexed by other letters, e.g. a_i. The first gate, $\mathfrak{U}_{\times,\mathbf{t}}$, controlled by x_6, sets:

$$\begin{aligned} a_1 &= y_2y_4y_6 + y_3y_4y_6 + y_2y_5y_6 + y_2y_3 + y_2y_4\\ &\quad + y_3y_5 + y_3y_6 + y_4y_6 + y_1 + y_3 + y_5,\\ a_2 &= y_4y_6 + y_3 + y_5 + y_6,\\ a_3 &= y_5y_6 + y_2 + y_4 + y_5 + y_6,\\ a_4 &= y_5,\\ a_5 &= y_4,\\ z_6 &= y_6 + 1. \end{aligned} \quad (20)$$

Then one acts with $\mathfrak{U}_{\times,\mathbf{u}_1}$ which is controlled by x_5:

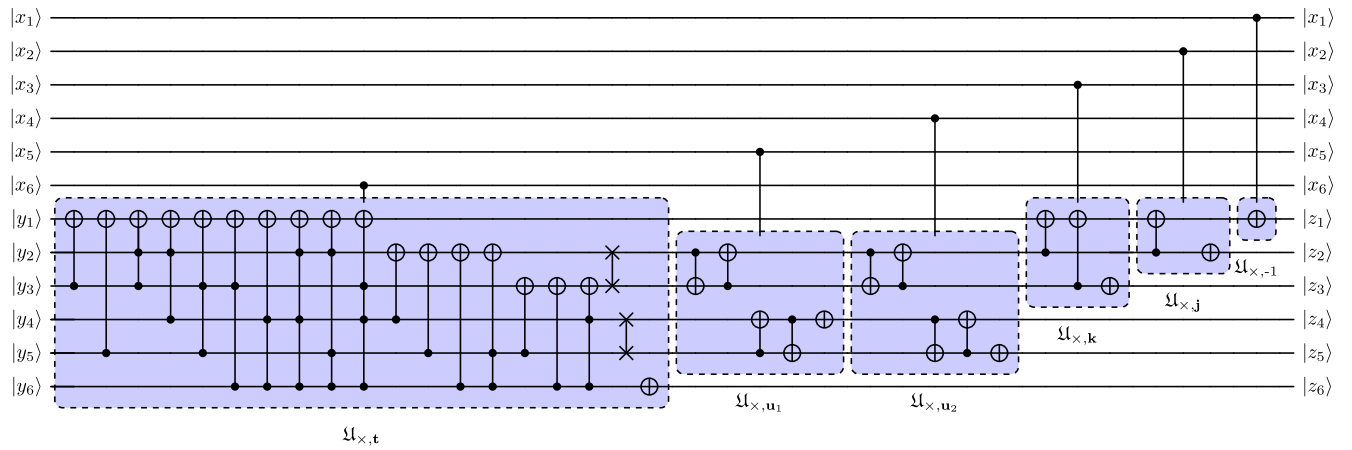

FIG. 4. The decomposition of the multiplication gate, $\mathfrak{U}_\times$, into a product of multiplication by each generator.

$$
\begin{aligned}
b_2 &= a_2 + a_3, \\
b_3 &= a_2, \\
b_4 &= a_5, \\
b_5 &= a_4 + a_5 + 1,
\end{aligned} \tag{21}
$$

where a_1 and z_6 do not change. Next, applying $\mathfrak{U}_{\times,\mathbf{u}_2}$ controlled by x_4,

$$
\begin{aligned}
c_2 &= b_3, \\
c_3 &= b_2 + b_3, \\
z_4 &= b_4 + b_5 + 1, \\
z_5 &= b_4,
\end{aligned} \tag{22}
$$

with a_1 and z_6 unchanged. $\mathfrak{U}_{\times,\mathbf{k}}$, controlled by x_3, sets

$$
\begin{aligned}
d_1 &= a_1 + c_2 + c_3, \\
z_3 &= c_3 + 1,
\end{aligned} \tag{23}
$$

where c_2, z_4, z_5, and z_6 are unchanged. Then, $\mathfrak{U}_{\times,\mathbf{j}}$ controlled by x_2 is

$$
\begin{aligned}
e_1 &= d_1 + c_2, \\
z_2 &= c_2 + 1,
\end{aligned} \tag{24}
$$

with z_3 through z_6 unchanged. Finally, $\mathfrak{U}_{\times,-1}$ needs $z_1 = e_1 + 1$ controlled by x_1 i.e. a CNOT. The full $\mathfrak{U}_\times$ is in Fig. 4.

VII. TRACE GATE

For simulating LGT, the Hamiltonian requires gauge-invariant operators. Without matter, all terms can be constructed from traces of g—and thus $\mathfrak{U}_{\mathrm{Tr}}$—in the fundamental irrep, ρ_4. Table I provides us with $\mathrm{ReTr}(g_i)$. In previous works [52,89,90], $\mathfrak{U}_{\mathrm{Tr}}$ was derived from a Hamiltonian, H_{Tr} with $\mathrm{ReTr}(g_i)$ as eigenvalues. For our $\mathbb{BO}$-register, H_{Tr} would require 20 Pauli strings which results in $\mathfrak{U}_{\mathrm{Tr}} = e^{i\theta H_{\mathrm{Tr}}}$ decomposing into at least 20 $R_Z(\theta)$ gates. In a fault-tolerant calculation, R_Z gates require synthesis from T gates, and thus can be unduly expensive.

Here, we explore a different implementation of $\mathfrak{U}_{\mathrm{Tr}}$ that is advantageous for discrete groups where $\mathrm{ReTr}(g)$ are limited by the number of conjugacy classes. In this case, $\mathfrak{U}_{\mathrm{Tr}}$ could be decomposed into two gates; a gate U_{conj} to map the 48 $|g\rangle$ to the 8 conjugacy classes $|c\rangle$, and a gate U_{Tr} which computes the traces for each conjugacy class. Together, we obtain a circuit for $\mathfrak{U}_{\mathrm{Tr}} = U_{\mathrm{conj}} U_{\mathrm{Tr}}(\theta) U_{\mathrm{conj}}^\dagger$ which should have fewer $R_Z(\theta)$ at the cost of additional C^{N}NOT gates which have ϵ-independent T gate costs. Taking the assignment of Table III for the traces we derive

$$
(-1)^{x_1} \mathbf{j}^{x_2} \mathbf{k}^{x_3} \mathbf{u}^{2x_4+x_5} \mathbf{t}^{x_6} \mapsto (v_1, v_2, v_3),
$$

where

$$
\begin{aligned}
v_1 &= (x_6+1)(x_1 + (x_4+x_5)(1+x_2)(1+x_3)) \\
&\quad + x_6(x_5x_1 + x_4(1+x_1) + (1+x_4+x_5)(x_2x_3+x_1)), \\
v_2 &= (x_6+1)((1+x_2)(1+x_3)(1+x_4+x_5)) \\
&\quad + x_6(x_5x_2 + x_4(1+x_3) + (1+x_4+x_5)(1+x_2+x_3)), \\
v_3 &= (x_6+1)(x_4+x_5) + x_6(x_5x_2 + x_4(1+x_3) \\
&\quad + (1+x_4+x_5)(1+x_2+x_3)).
\end{aligned} \tag{25}
$$

TABLE III. Trace elements and associated bit strings for the conjugacy classes stored in the ancilla. Note, v_1 is a sign bit.

$\mathrm{Re\,Tr}\,(g)$	0	0	2	−2	1	−1	$\sqrt{2}$	$-\sqrt{2}$
$v1$	0	1	0	1	0	1	0	1
$v2$	0	0	1	1	0	0	1	1
$v3$	0	0	0	0	1	1	1	1

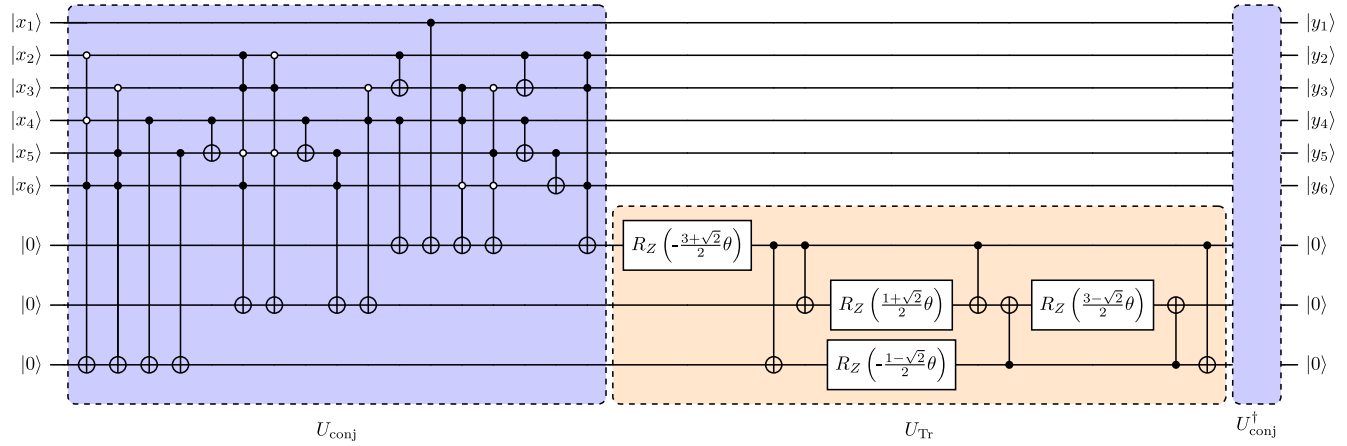

FIG. 5. A qubit implementation of $\mathfrak{U}_{\text{Tr}}$.

A qubit-based circuit for $\mathfrak{U}_{\text{Tr}}$ is shown in Fig. 5. With this, we will estimate the reduction in fault-tolerant resource gate costs in Sec. IX compared to the H_{Tr} method.

VIII. FOURIER TRANSFORM

The standard n-qubit quantum Fourier transform (QFT) [166] corresponds to the quantum version of the fast Fourier transform of $\mathbb{Z}_{2^n}$. Quantum Fourier transforms over some non-Abelian groups exist [89,167–170]. Alas, for the crystal-like subgroups, efficient QFT circuits are currently unknown [171]. In general, no clear algorithmic way to construct the QFT exists. Thus, we instead construct a suboptimal $\mathfrak{U}_F$ from Eq. (8) from the irreps.

Since $\mathbb{BO}$ has 48 elements, on a qubit device $\mathfrak{U}_F$ must be embedded into a larger $2^d \times 2^d$ unitary. The columns index qubit bitstrings from $|0\rangle$ to $|63\rangle$ where the physical states are given by the subset of $|g\rangle$ in Table I. We then index the irreducible representation ρ_i sequentially from $i = 1$ to $i = 8$, and construct the matrix, including appropriate padding for the forbidden states. This matrix was then passed to the Qiskit v0.43.1 transpiler, and an optimized version of $\mathfrak{U}_F$ needed 1839 CNOTs, 166 R_X, 1996 R_Y, and 3401 R_Z gates[1]; the Fourier gate is the most expensive qubit primitive and dominates simulation costs.

IX. RESOURCE ESTIMATES

Clearly quantum practicality with $\mathbb{BO}$ will require error corrections. Since the Eastin-Knill theorem restricts QEC codes from having a universal transversal sets of gates [172], compromises must be made. Typically, the Clifford gates are transversal [173–177] while the T gate is not. Thus T gate counts are often used in fault-tolerant resource analysis [173,178]. Recently, novel universal sets have been proposed with transversal $\mathbb{BT}, \mathbb{BO}, \mathbb{BI}$ gates [179–182] which deserve investigation for use with LGT.

The Toffoli gate requires 7 T gates [173] and one method for constructing the C^{n}NOT gates is with $2\lceil \log_2 n \rceil - 1$ Toffoli gates and $n-2$ dirty ancilla qubits[2] which can be reused later [173,183,184]. We arrive at the cost for the R_Z gates via [185] where these gates can be approximated to precision ϵ with on average $1.15\log_2(1/\epsilon)$ T gates (and at worst $-9 + 4\log_2(1/\epsilon)$ [186]). Further, R_Y and R_X can be replaced by at most 3 R_Z. With these, we can construct gate estimates for $\mathbb{BO}$ (See Table IV). We note that for $\epsilon \lesssim 10^{-6}$, the 20 $R_Z(\theta)$ required for $e^{i\theta H_{\text{Tr}}}$ is more expensive than the $\mathfrak{U}_{\text{Tr}}$ constructed using U_{conj}.

Primitive gate costs for implementing H_{KS} [164] and H_I [80], per link per Trotter step δt are shown in Table V. Using these, we can determine the total T gate count $N_T^H = C_T^H \times dL^d N_t$ for a d spatial lattice simulated for a time $t = N_t \delta t$. We find that for H_{KS}

$$C_T^{\text{KS}} = 2863(d-1) + (22737.8 + 2.3d)\log_2 \frac{1}{\epsilon}. \quad (26)$$

With this, the total synthesis error ϵ_T can be estimated as the sum of ϵ from each R_Z. In the case of H_{KS} this is

$$\epsilon_T = 2(9886 + d)dL^d N_t \times \epsilon. \quad (27)$$

If one looks to reduce lattice spacing errors for a fixed number of qubits, one can use H_I which would require

$$C_T^I = 11949d - 10157 + (45473.3 + 6.9d)\log_2 \frac{1}{\epsilon}, \quad (28)$$

where the total synthesis error is

[1]In [90], the Qiskit v0.37.2 was used, yielding for the $\mathbb{BT}$ $\mathfrak{U}_F$ of 1025 CNOTs, 1109 R_Y, and 2139 R_Z gates. With the v0.43.1 transpiler, we obtain 442 CNOTs, 40 R_X, 494 R_Y, and 835 R_Z.

[2]A *clean* ancilla is in state $|0\rangle$. *Dirty* ancillae have unknown states.

TABLE IV. Number of physical T gates and clean ancilla required to implement logical gates for (top) basic gates taken from [173] (bottom) primitive gates for $\mathbb{BO}$.

Gate	T gates	Clean ancilla
C^2NOT	7	0
C^3NOT	21	1
C^4NOT	35	2
CSWAP	7	0
R_Z	$1.15\ \log_2(1/\epsilon)$	0
$\mathcal{U}_{-1}$	112	1
$\mathcal{U}_{\times}$	392	4
$\mathcal{U}_{\mathrm{Tr}}$	340[a]+$4.6\log_2(1/\epsilon)$	2
$\mathcal{U}_{FT}$	$11370.1\ \log_2(1/\epsilon)$	0

[a]With 6 additional ancilla, this can be reduced to 188.

TABLE V. Number of primitive gates per link per δt neglecting boundary effects as a function of d for H_{KS} and H_I.

Gate	$N[H_{\mathrm{KS}}]$	$N[H_I]$
$\mathfrak{U}_F$	2	4
$\mathfrak{U}_{\mathrm{Tr}}$	$\frac{1}{2}(d-1)$	$\frac{3}{2}(d-1)$
$\mathfrak{U}_{-1}$	$3(d-1)$	$2+11(d-1)$
$\mathfrak{U}_{\times}$	$6(d-1)$	$4+26(d-1)$

$$\epsilon_T = 2(19771+3d)dL^dN_t \times \epsilon. \tag{29}$$

Following [57,90,143], we will make resource estimates based on our primitive gates for the calculation of the shear viscosity η on a $L^3 = 10^3$ lattice evolved for $N_t = 50$, and total synthesis error of $\epsilon_T = 10^{-8}$. Considering only the time evolution and neglecting state preparation (which can be substantial [12,14,17–21,28,30–33,51,82,84,87,187]), Kan and Nam estimated 3×10^{19} T gates would be required for an pure-gauge $SU(2)$ simulation of H_{KS}. This estimate used a truncated electric-field digitization which requires substantial fixed-point arithmetic—greatly inflating the T gate cost. Using $\mathbb{BT}$, we presently estimate that 1.1×10^{11} T gates would be sufficient[3] but only H_I could be used. Here, the $\mathbb{BO}$ group would require 4.1×10^{11} T gates if H_I were used—albeit with smaller lattice spacing errors than Kan and Nam since they used H_{KS}. Thus $\mathbb{BO}$ reduces the gate costs of [143] by 10^8 for fixed L by avoiding quantum fixed-point arithmetic while allowing for smaller lattice spacings that $\mathbb{BT}$. If H_{KS} were used the T gate cost is reduced to 2.0×10^{11}. Alternatively, if we take the heuristic of [80] that for $a = \mathcal{O}(0.1\ \mathrm{fm})$ using H_I could reduce L by half for fixed lattice spacing errors with only 4.9×10^{10} T gates. Similar to $\mathbb{BT}$, $\mathfrak{U}_F$ dominates the simulations—99% and 98% of the total cost of simulation H_{KS} and H_I, respectively.

[3]This supersedes [90] due to the improved transpiler, proper consideration of ϵ_T, and better cost estimates of R_X, R_Y.

X. CONCLUSIONS

In this paper, we constructed the necessary primitive gates for the simulation of $\mathbb{BO}$—a crystal-like subgroup of $SU(2)$—gauge theories and quantum resource estimates were made for the simulation of pure $SU(2)$ shear viscosity. Compared to previous fault-tolerant qubit estimates of electric basis truncations, we require 10^8 fewer T gates by avoiding quantum fixed point arithmetic via the discrete group approximation. Further, reducing digitization error compared to $\mathbb{BT}$ increase the total cost by a factor of ~ 4 perhaps suggesting a $|G|^2$ scaling.

Looking forward, primitive gates should be constructed for $\mathbb{BI}$ and to the subgroups of $SU(3)$. At the cost of more qubits, $\mathbb{BI}$ would allow smaller digitization error and lattice spacings. To further reduce the qubit-based simulation gate costs for all discrete subgroup approximations, the formalism for deriving the quantum Fourier transform for crystal-like groups remains of paramount interest.

ACKNOWLEDGMENTS

The authors thank M. S. Alam, N. Suri, R. Van de Water and M. Wagman for insightful comments and support over the course of this work. E. G. was supported by the NASA Academic Mission Services, Contract No. NNA16BD14C. H. L. and F. L. are supported by the Department of Energy through the Fermilab QuantiSED program in the area of "Intersections of QIS and Theoretical Particle Physics." This material is based on work supported by the U.S. Department of Energy, Office of Science, National Quantum Information Science Research Centers, Superconducting Quantum Materials and Systems Center (SQMS) under Contract No. DE-AC02-07CH11359 (E. G.). Fermilab is operated by Fermi Research Alliance, LLC under Contract No. DE-AC02-07CH11359 with the United States Department of Energy.

[1] N. Klco, A. Roggero, and M. J. Savage, Standard model physics and the digital quantum revolution: Thoughts about the interface, Rep. Prog. Phys. **85**, 064301 (2022).

[2] M. C. Bañuls *et al.*, Simulating lattice gauge theories within quantum technologies, Eur. Phys. J. D **74**, 165 (2020).

[3] C. W. Bauer *et al.*, Quantum simulation for high-energy physics, PRX Quantum **4**, 027001 (2023).

[4] A. Di Meglio *et al.*, Quantum computing for high-energy physics: State of the art and challenges. Summary of the QC4HEP working group, arXiv:2307.03236.

[5] C. Gattringer and K. Langfeld, Approaches to the sign problem in lattice field theory, Int. J. Mod. Phys. A **31**, 1643007 (2016).

[6] S. Kühn, J. I. Cirac, and M.-C. Bañuls, Quantum simulation of the Schwinger model: A study of feasibility, Phys. Rev. A **90**, 042305 (2014).

[7] C. Kokail *et al.*, Self-verifying variational quantum simulation of the lattice Schwinger model, Nature (London) **569**, 355 (2019).

[8] B. Chakraborty, M. Honda, T. Izubuchi, Y. Kikuchi, and A. Tomiya, Classically emulated digital quantum simulation of the Schwinger model with a topological term via adiabatic state preparation, Phys. Rev. D **105**, 094503 (2022).

[9] A. Yamamoto, Quantum variational approach to lattice gauge theory at nonzero density, Phys. Rev. D **104**, 014506 (2021).

[10] R. Desai, Y. Feng, M. Hassan, A. Kodumagulla, and M. McGuigan, Z3 gauge theory coupled to fermions and quantum computing, arXiv:2106.00549.

[11] R. C. Farrell, M. Illa, A. N. Ciavarella, and M. J. Savage, Scalable circuits for preparing ground states on digital quantum computers: The Schwinger model vacuum on 100 qubits, arXiv:2308.04481.

[12] C. F. Kane, N. Gomes, and M. Kreshchuk, Nearly-optimal state preparation for quantum simulations of lattice gauge theories, arXiv:2310.13757.

[13] E. Bilgin and S. Boixo, Preparing thermal states of quantum systems by dimension reduction, Phys. Rev. Lett. **105**, 170405 (2010).

[14] A. Riera, C. Gogolin, and J. Eisert, Thermalization in nature and on a quantum computer, Phys. Rev. Lett. **108**, 080402 (2012).

[15] H. Lamm and S. Lawrence, Simulation of nonequilibrium dynamics on a quantum computer, Phys. Rev. Lett. **121**, 170501 (2018).

[16] N. Klco and M. J. Savage, Minimally-entangled state preparation of localized wavefunctions on quantum computers, Phys. Rev. A **102**, 012612 (2020).

[17] S. Harmalkar, H. Lamm, and S. Lawrence (NuQS Collaboration), Quantum simulation of field theories without state preparation, arXiv:2001.11490.

[18] M. Motta, C. Sun, A. T. Tan, M. J. O'Rourke, E. Ye, A. J. Minnich, F. G. Brandao, and G. K.-L. Chan, Determining eigenstates and thermal states on a quantum computer using quantum imaginary time evolution, Nat. Phys. **16**, 205 (2020).

[19] W. A. de Jong, K. Lee, J. Mulligan, M. Płoskoń, F. Ringer, and X. Yao, Quantum simulation of non-equilibrium dynamics and thermalization in the Schwinger model, Phys. Rev. D **106**, 054508 (2022).

[20] X.-D. Xie, X. Guo, H. Xing, Z.-Y. Xue, D.-B. Zhang, and S.-L. Zhu (QuNu Collaboration), Variational thermal quantum simulation of the lattice Schwinger model, Phys. Rev. D **106**, 054509 (2022).

[21] Z. Davoudi, N. Mueller, and C. Powers, Towards quantum computing phase diagrams of gauge theories with thermal pure quantum states, Phys. Rev. Lett. **131**, 081901 (2023).

[22] C. Ball and T. D. Cohen, Boltzmann distributions on a quantum computer via active cooling, Nucl. Phys. **A1038**, 122708 (2023).

[23] J. Saroni, H. Lamm, P. P. Orth, and T. Iadecola, Reconstructing thermal quantum quench dynamics from pure states, Phys. Rev. B **108**, 134301 (2023).

[24] S. P. Jordan, K. S. M. Lee, and J. Preskill, Quantum algorithms for quantum field theories, Science **336**, 1130 (2012).

[25] S. P. Jordan, K. S. M. Lee, and J. Preskill, Quantum computation of scattering in scalar quantum field theories, Quantum Inf. Comput. **14**, 1014 (2014).

[26] L. García-Álvarez, J. Casanova, A. Mezzacapo, I. L. Egusquiza, L. Lamata, G. Romero, and E. Solano, Fermion-fermion scattering in quantum field theory with superconducting circuits, Phys. Rev. Lett. **114**, 070502 (2015).

[27] S. P. Jordan, K. S. M. Lee, and J. Preskill, Quantum algorithms for fermionic quantum field theories, arXiv:1404.7115.

[28] S. P. Jordan, H. Krovi, K. S. Lee, and J. Preskill, BQP-completeness of scattering in scalar quantum field theory, Quantum **2**, 44 (2018).

[29] A. Hamed Moosavian and S. Jordan, Faster quantum algorithm to simulate fermionic quantum field theory, Phys. Rev. A **98**, 012332 (2018).

[30] F. G. Brandão and M. J. Kastoryano, Finite correlation length implies efficient preparation of quantum thermal states, Commun. Math. Phys. **365**, 1 (2019).

[31] E. Gustafson, Y. Meurice, and J. Unmuth-Yockey, Quantum simulation of scattering in the quantum Ising model, Phys. Rev. D **99**, 094503 (2019).

[32] E. Gustafson, P. Dreher, Z. Hang, and Y. Meurice, Benchmarking quantum computers for real-time evolution of a $(1+1)$ field theory with error mitigation, Quantum Sci. Technol. **6**, 045020 (2021).

[33] E. J. Gustafson and H. Lamm, Toward quantum simulations of $\mathbb{Z}_2$ gauge theory without state preparation, Phys. Rev. D **103**, 054507 (2021).

[34] M. Kreshchuk, J. P. Vary, and P. J. Love, Simulating scattering of composite particles, arXiv:2310.13742.

[35] A. M. Childs, Y. Su, M. C. Tran, N. Wiebe, and S. Zhu, Theory of Trotter error with commutator scaling, Phys. Rev. X **11**, 011020 (2021).

[36] Z. Davoudi, A. F. Shaw, and J. R. Stryker, General quantum algorithms for Hamiltonian simulation with applications to a non-Abelian lattice gauge theory, Quantum **7**, 1213 (2023).

[37] E. Campbell, Random compiler for fast Hamiltonian simulation, Phys. Rev. Lett. **123**, 070503 (2019).

[38] A. F. Shaw, P. Lougovski, J. R. Stryker, and N. Wiebe, Quantum algorithms for simulating the lattice Schwinger model, Quantum **4**, 306 (2020).
[39] D. W. Berry, A. M. Childs, R. Cleve, R. Kothari, and R. D. Somma, Simulating Hamiltonian dynamics with a truncated Taylor series, Phys. Rev. Lett. **114**, 090502 (2015).
[40] G. H. Low and I. L. Chuang, Hamiltonian simulation by qubitization, Quantum **3**, 163 (2019).
[41] D. W. Berry and A. M. Childs, Black-box Hamiltonian simulation and unitary implementation, Quantum Inf. Comput. **12** (2012).
[42] G. H. Low and I. L. Chuang, Optimal Hamiltonian simulation by quantum signal processing, Phys. Rev. Lett. **118**, 010501 (2017).
[43] A. M. Childs and N. Wiebe, Hamiltonian simulation using linear combinations of unitary operations, Quantum Inf. Comput. **12**, 901 (2012).
[44] C. Cirstoiu, Z. Holmes, J. Iosue, L. Cincio, P. J. Coles, and A. Sornborger, Variational fast forwarding for quantum simulation beyond the coherence time, npj Quantum Inf. **6**, 1 (2020).
[45] J. Gibbs, K. Gili, Z. Holmes, B. Commeau, A. Arrasmith, L. Cincio, P. J. Coles, and A. Sornborger, Long-time simulations with high fidelity on quantum hardware, arXiv:2102.04313.
[46] Y.-X. Yao, N. Gomes, F. Zhang, C.-Z. Wang, K.-M. Ho, T. Iadecola, and P. P. Orth, Adaptive variational quantum dynamics simulations, PRX Quantum **2**, 030307 (2021).
[47] L. Nagano, A. Bapat, and C. W. Bauer, Quench dynamics of the Schwinger model via variational quantum algorithms, Phys. Rev. D **108**, 034501 (2023).
[48] A. Roggero and J. Carlson, Linear response on a quantum computer, Phys. Rev. C **100**, 034610 (2019).
[49] A. Roggero and A. Baroni, Short-depth circuits for efficient expectation value estimation, Phys. Rev. A **101**, 022328 (2020).
[50] S. Kanasugi, S. Tsutsui, Y. O. Nakagawa, K. Maruyama, H. Oshima, and S. Sato, Computation of Green's function by local variational quantum compilation, Phys. Rev. Res. **5**, 033070 (2023).
[51] E. J. Gustafson, H. Lamm, and J. Unmuth-Yockey, Quantum mean estimation for lattice field theory, Phys. Rev. D **107**, 114511 (2023).
[52] H. Lamm, S. Lawrence, and Y. Yamauchi (NuQS Collaboration), General methods for digital quantum simulation of gauge theories, Phys. Rev. D **100**, 034518 (2019).
[53] C. W. Bauer, W. A. de Jong, B. Nachman, and D. Provasoli, Quantum algorithm for high energy physics simulations, Phys. Rev. Lett. **126**, 062001 (2021).
[54] M. Echevarria, I. Egusquiza, E. Rico, and G. Schnell, Quantum simulation of light-front parton correlators, Phys. Rev. D **104**, 014512 (2021).
[55] B. Xu and W. Xue, $(3+1)$-dimensional Schwinger pair production with quantum computers, Phys. Rev. D **106**, 116007 (2022).
[56] C. W. Bauer, M. Freytsis, and B. Nachman, Simulating collider physics on quantum computers using effective field theories, Phys. Rev. Lett. **127**, 212001 (2021).
[57] T. D. Cohen, H. Lamm, S. Lawrence, and Y. Yamauchi (NuQS Collaboration), Quantum algorithms for transport coefficients in gauge theories, Phys. Rev. D **104**, 094514 (2021).
[58] J. a. Barata, X. Du, M. Li, W. Qian, and C. A. Salgado, Medium induced jet broadening in a quantum computer, Phys. Rev. D **106**, 074013 (2022).
[59] A. M. Czajka, Z.-B. Kang, Y. Tee, and F. Zhao, Studying chirality imbalance with quantum algorithms, arXiv:2210.03062.
[60] R. C. Farrell, I. A. Chernyshev, S. J. M. Powell, N. A. Zemlevskiy, M. Illa, and M. J. Savage, Preparations for quantum simulations of quantum chromodynamics in $1+1$ dimensions. II. Single-baryon β-decay in real time, Phys. Rev. D **107**, 054513 (2023).
[61] P. F. Bedaque, R. Khadka, G. Rupak, and M. Yusf, Radiative processes on a quantum computer, arXiv:2209.09962.
[62] K. Ikeda, D. E. Kharzeev, R. Meyer, and S. Shi, Detecting the critical point through entanglement in Schwinger model, Phys. Rev. D **108**, L091501 (2023).
[63] A. Ciavarella, Algorithm for quantum computation of particle decays, Phys. Rev. D **102**, 094505 (2020).
[64] E. Huffman, M. García Vera, and D. Banerjee, Toward the real-time evolution of gauge-invariant $\mathbb{Z}_2$ and $U(1)$ quantum link models on noisy intermediate-scale quantum hardware with error mitigation, Phys. Rev. D **106**, 094502 (2022).
[65] N. Klco and M. J. Savage, Hierarchical qubit maps and hierarchically implemented quantum error correction, Phys. Rev. A **104**, 062425 (2021).
[66] C. Charles, E. J. Gustafson, E. Hardt, F. Herren, N. Hogan, H. Lamm, S. Starecheski, R. S. Van de Water, and M. L. Wagman, Simulating $\mathbb{Z}_2$ lattice gauge theory on a quantum computer, Phys. Rev. E **109**, 015307 (2024).
[67] E. Gustafson, Noise improvements in quantum simulations of sQED using qutrits, arXiv:2201.04546.
[68] A. Rajput, A. Roggero, and N. Wiebe, Quantum error correction with gauge symmetries, npj Quantum Inf. **9**, 41 (2023).
[69] E. J. Gustafson and H. Lamm, Robustness of gauge digitization to quantum noise, arXiv:2301.10207.
[70] J. C. Halimeh and P. Hauke, Reliability of lattice gauge theories, Phys. Rev. Lett. **125**, 030503 (2020).
[71] H. Lamm, S. Lawrence, and Y. Yamauchi (NuQS Collaboration), Suppressing coherent gauge drift in quantum simulations, arXiv:2005.12688.
[72] M. C. Tran, Y. Su, D. Carney, and J. M. Taylor, Faster digital quantum simulation by symmetry protection, PRX Quantum **2**, 010323 (2021).
[73] V. Kasper, T. V. Zache, F. Jendrzejewski, M. Lewenstein, and E. Zohar, Non-Abelian gauge invariance from dynamical decoupling, Phys. Rev. D **107**, 014506 (2023).
[74] J. C. Halimeh, H. Lang, J. Mildenberger, Z. Jiang, and P. Hauke, Gauge-symmetry protection using single-body terms, PRX Quantum **2**, 040311 (2021).
[75] M. Van Damme, J. C. Halimeh, and P. Hauke, Gauge-symmetry violation quantum phase transition in lattice gauge theories, arXiv:2010.07338.

[76] N. H. Nguyen, M. C. Tran, Y. Zhu, A. M. Green, C. H. Alderete, Z. Davoudi, and N. M. Linke, Digital quantum simulation of the Schwinger model and symmetry protection with trapped ions, PRX Quantum **3**, 020324 (2022).
[77] J. C. Halimeh, H. Lang, and P. Hauke, Gauge protection in non-Abelian lattice gauge theories, New J. Phys. **24**, 033015 (2022).
[78] S. A Rahman, R. Lewis, E. Mendicelli, and S. Powell, Self-mitigating Trotter circuits for SU(2) lattice gauge theory on a quantum computer, Phys. Rev. D **106**, 074502 (2022).
[79] K. Yeter-Aydeniz, Z. Parks, A. Nair, E. Gustafson, A. F. Kemper, R. C. Pooser, Y. Meurice, and P. Dreher, Measuring NISQ gate-based qubit stability using a $1+1$ field theory and cycle benchmarking, Quantum Inf. Process. **22**, 96 (2023).
[80] M. Carena, H. Lamm, Y.-Y. Li, and W. Liu, Improved Hamiltonians for quantum simulations, Phys. Rev. Lett. **129**, 051601 (2022).
[81] A. N. Ciavarella, Quantum simulation of lattice QCD with improved Hamiltonians, Phys. Rev. D **108**, 094513 (2023).
[82] E. J. Gustafson, Stout smearing on a quantum computer, arXiv:2211.05607.
[83] K. Temme, T. Osborne, K. Vollbrecht, D. Poulin, and F. Verstraete, Quantum metropolis sampling, Nature (London) **471**, 87 (2011).
[84] G. Clemente *et al.* (QuBiPF Collaboration), Quantum computation of thermal averages in the presence of a sign problem, Phys. Rev. D **101**, 074510 (2020).
[85] A. Yamamoto, Quantum sampling for the Euclidean path integral of lattice gauge theory, Phys. Rev. D **105**, 094501 (2022).
[86] E. Ballini, G. Clemente, M. D'Elia, L. Maio, and K. Zambello, Quantum computation of thermal averages for a non-Abelian D_4 lattice gauge theory via quantum metropolis sampling, arXiv:2309.07090.
[87] A. Avkhadiev, P. E. Shanahan, and R. D. Young, Accelerating lattice quantum field theory calculations via interpolator optimization using noisy intermediate-scale quantum computing, Phys. Rev. Lett. **124**, 080501 (2020).
[88] A. Avkhadiev, P. E. Shanahan, and R. D. Young, Strategies for quantum-optimized construction of interpolating operators in classical simulations of lattice quantum field theories, Phys. Rev. D **107**, 054507 (2023).
[89] M. S. Alam, S. Hadfield, H. Lamm, and A. C. Y. Li (SQMS Collaboration), Primitive quantum gates for dihedral gauge theories, Phys. Rev. D **105**, 114501 (2022).
[90] E. J. Gustafson, H. Lamm, F. Lovelace, and D. Musk, Primitive quantum gates for an SU(2) discrete subgroup: Binary tetrahedral, Phys. Rev. D **106**, 114501 (2022).
[91] T. V. Zache, D. González-Cuadra, and P. Zoller, Quantum and classical spin-network algorithms for q-deformed Kogut-Susskind gauge theories, Phys. Rev. Lett. **131**, 171902 (2023).
[92] T. V. Zache, D. González-Cuadra, and P. Zoller, Fermion-qudit quantum processors for simulating lattice gauge theories with matter, Quantum **7**, 1140 (2023).
[93] E. Zohar, J. I. Cirac, and B. Reznik, Simulating compact quantum electrodynamics with ultracold atoms: Probing confinement and nonperturbative effects, Phys. Rev. Lett. **109**, 125302 (2012).
[94] E. Zohar, J. I. Cirac, and B. Reznik, Cold-atom quantum simulator for SU(2) Yang-Mills lattice gauge theory, Phys. Rev. Lett. **110**, 125304 (2013).
[95] E. Zohar, J. I. Cirac, and B. Reznik, Quantum simulations of gauge theories with ultracold atoms: Local gauge invariance from angular momentum conservation, Phys. Rev. A **88**, 023617 (2013).
[96] E. Zohar and M. Burrello, Formulation of lattice gauge theories for quantum simulations, Phys. Rev. D **91**, 054506 (2015).
[97] E. Zohar, J. I. Cirac, and B. Reznik, Quantum simulations of lattice gauge theories using ultracold atoms in optical lattices, Rep. Prog. Phys. **79**, 014401 (2016).
[98] E. Zohar, A. Farace, B. Reznik, and J. I. Cirac, Digital lattice gauge theories, Phys. Rev. A **95**, 023604 (2017).
[99] N. Klco, J. R. Stryker, and M. J. Savage, SU(2) non-Abelian gauge field theory in one dimension on digital quantum computers, Phys. Rev. D **101**, 074512 (2020).
[100] A. Ciavarella, N. Klco, and M. J. Savage, A trailhead for quantum simulation of SU(3) Yang-Mills lattice gauge theory in the local multiplet basis, Phys. Rev. D **103**, 094501 (2021).
[101] J. Bender, E. Zohar, A. Farace, and J. I. Cirac, Digital quantum simulation of lattice gauge theories in three spatial dimensions, New J. Phys. **20**, 093001 (2018).
[102] J. Liu and Y. Xin, Quantum simulation of quantum field theories as quantum chemistry, J. High Energy Phys. 12 (2020) 011.
[103] D. C. Hackett, K. Howe, C. Hughes, W. Jay, E. T. Neil, and J. N. Simone, Digitizing gauge fields: Lattice Monte Carlo results for future quantum computers, Phys. Rev. A **99**, 062341 (2019).
[104] A. Alexandru, P. F. Bedaque, S. Harmalkar, H. Lamm, S. Lawrence, and N. C. Warrington (NuQS Collaboration), Gluon field digitization for quantum computers, Phys. Rev. D **100**, 114501 (2019).
[105] A. Yamamoto, Real-time simulation of $(2+1)$-dimensional lattice gauge theory on qubits, Prog. Theor. Exp. Phys. **2021**, 013B06 (2021).
[106] J. F. Haase, L. Dellantonio, A. Celi, D. Paulson, A. Kan, K. Jansen, and C. A. Muschik, A resource efficient approach for quantum and classical simulations of gauge theories in particle physics, Quantum **5**, 393 (2021).
[107] T. Armon, S. Ashkenazi, G. García-Moreno, A. González-Tudela, and E. Zohar, Photon-mediated stroboscopic quantum simulation of a $\mathbb{Z}_2$ lattice gauge theory, Phys. Rev. Lett. **127**, 250501 (2021).
[108] A. Bazavov, S. Catterall, R. G. Jha, and J. Unmuth-Yockey, Tensor renormalization group study of the non-Abelian Higgs model in two dimensions, Phys. Rev. D **99**, 114507 (2019).
[109] A. Bazavov, Y. Meurice, S.-W. Tsai, J. Unmuth-Yockey, and J. Zhang, Gauge-invariant implementation of the

Abelian Higgs model on optical lattices, Phys. Rev. D **92**, 076003 (2015).
[110] J. Zhang, J. Unmuth-Yockey, J. Zeiher, A. Bazavov, S. W. Tsai, and Y. Meurice, Quantum simulation of the universal features of the Polyakov loop, Phys. Rev. Lett. **121**, 223201 (2018).
[111] J. Unmuth-Yockey, J. Zhang, A. Bazavov, Y. Meurice, and S.-W. Tsai, Universal features of the Abelian Polyakov loop in $1+1$ dimensions, Phys. Rev. D **98**, 094511 (2018).
[112] J. F. Unmuth-Yockey, Gauge-invariant rotor Hamiltonian from dual variables of 3D $U(1)$ gauge theory, Phys. Rev. D **99**, 074502 (2019).
[113] M. Kreshchuk, W. M. Kirby, G. Goldstein, H. Beauchemin, and P. J. Love, Quantum simulation of quantum field theory in the light-front formulation, Phys. Rev. A **105**, 032418 (2022).
[114] M. Kreshchuk, S. Jia, W. M. Kirby, G. Goldstein, J. P. Vary, and P. J. Love, Simulating hadronic physics on NISQ devices using basis light-front quantization, Phys. Rev. A **103**, 062601 (2021).
[115] I. Raychowdhury and J. R. Stryker, Solving Gauss's law on digital quantum computers with loop-string-hadron digitization, Phys. Rev. Res. **2**, 033039 (2020).
[116] I. Raychowdhury and J. R. Stryker, Loop, string, and hadron dynamics in SU(2) Hamiltonian lattice gauge theories, Phys. Rev. D **101**, 114502 (2020).
[117] Z. Davoudi, I. Raychowdhury, and A. Shaw, Search for efficient formulations for Hamiltonian simulation of non-Abelian lattice gauge theories, Phys. Rev. D **104**, 074505 (2021).
[118] U.-J. Wiese, Towards quantum simulating QCD, Nucl. Phys. **A931**, 246 (2014).
[119] D. Luo, J. Shen, M. Highman, B. K. Clark, B. DeMarco, A. X. El-Khadra, and B. Gadway, A framework for simulating gauge theories with dipolar spin systems, Phys. Rev. A **102**, 032617 (2020).
[120] R. C. Brower, D. Berenstein, and H. Kawai, Lattice gauge theory for a quantum computer, Proc. Sci. LATTICE2019 (**2019**) 112 [arXiv:2002.10028].
[121] S. V. Mathis, G. Mazzola, and I. Tavernelli, Toward scalable simulations of lattice gauge theories on quantum computers, Phys. Rev. D **102**, 094501 (2020).
[122] H. Singh, Qubit $O(N)$ nonlinear sigma models, Phys. Rev. D **105**, 114509 (2022).
[123] H. Singh and S. Chandrasekharan, Qubit regularization of the $O(3)$ sigma model, Phys. Rev. D **100**, 054505 (2019).
[124] A. J. Buser, T. Bhattacharya, L. Cincio, and R. Gupta, State preparation and measurement in a quantum simulation of the $O(3)$ sigma model, Phys. Rev. D **102**, 114514 (2020).
[125] T. Bhattacharya, A. J. Buser, S. Chandrasekharan, R. Gupta, and H. Singh, Qubit regularization of asymptotic freedom, Phys. Rev. Lett. **126**, 172001 (2021).
[126] J. Barata, N. Mueller, A. Tarasov, and R. Venugopalan, Single-particle digitization strategy for quantum computation of a ϕ^4 scalar field theory, Phys. Rev. A **103**, 042410 (2021).
[127] M. Kreshchuk, S. Jia, W. M. Kirby, G. Goldstein, J. P. Vary, and P. J. Love, Light-front field theory on current quantum computers, Entropy **23**, 597 (2021).
[128] Y. Ji, H. Lamm, and S. Zhu (NuQS Collaboration), Gluon field digitization via group space decimation for quantum computers, Phys. Rev. D **102**, 114513 (2020).
[129] C. W. Bauer and D. M. Grabowska, Efficient representation for simulating U(1) gauge theories on digital quantum computers at all values of the coupling, Phys. Rev. D **107**, L031503 (2023).
[130] E. Gustafson, Prospects for simulating a qudit based model of $(1+1)$D scalar QED, Phys. Rev. D **103**, 114505 (2021).
[131] T. Hartung, T. Jakobs, K. Jansen, J. Ostmeyer, and C. Urbach, Digitising SU(2) gauge fields and the freezing transition, Eur. Phys. J. C **82**, 237 (2022).
[132] D. M. Grabowska, C. Kane, B. Nachman, and C. W. Bauer, Overcoming exponential scaling with system size in Trotter-Suzuki implementations of constrained Hamiltonians: $2+1$ U(1) lattice gauge theories, arXiv:2208.03333.
[133] E. M. Murairi, M. J. Cervia, H. Kumar, P. F. Bedaque, and A. Alexandru, How many quantum gates do gauge theories require?, Phys. Rev. D **106**, 094504 (2022).
[134] P. Hasenfratz and F. Niedermayer, Asymptotic freedom with discrete spin variables?, Proc. Sci. HEP2001 (**2001**) 229 [arXiv:hep-lat/0112003].
[135] S. Caracciolo, A. Montanari, and A. Pelissetto, Asymptotically free models and discrete non-Abelian groups, Phys. Lett. B **513**, 223 (2001).
[136] P. Hasenfratz and F. Niedermayer, Asymptotically free theories based on discrete subgroups, Nucl. Phys. B, Proc. Suppl. **94**, 575 (2001).
[137] A. Patrascioiu and E. Seiler, Continuum limit of two-dimensional spin models with continuous symmetry and conformal quantum field theory, Phys. Rev. E **57**, 111 (1998).
[138] R. Krcmar, A. Gendiar, and T. Nishino, Phase diagram of a truncated tetrahedral model, Phys. Rev. E **94**, 022134 (2016).
[139] S. Caracciolo, A. Montanari, and A. Pelissetto, Asymptotically free models and discrete non-Abelian groups, Phys. Lett. B **513**, 223 (2001).
[140] J. Zhou, H. Singh, T. Bhattacharya, S. Chandrasekharan, and R. Gupta, Spacetime symmetric qubit regularization of the asymptotically free two-dimensional O(4) model, Phys. Rev. D **105**, 054510 (2022).
[141] S. Caspar and H. Singh, From asymptotic freedom to θ vacua: Qubit embeddings of the O(3) nonlinear σ model, Phys. Rev. Lett. **129**, 022003 (2022).
[142] E. Zohar, Quantum simulation of lattice gauge theories in more than one space dimension—requirements, challenges, methods, Phil. Trans. R. Soc. A **380**, 20210069 (2021).
[143] A. Kan and Y. Nam, Lattice quantum chromodynamics and electrodynamics on a universal quantum computer, arXiv:2107.12769.
[144] M. Carena, H. Lamm, Y.-Y. Li, and W. Liu, Lattice renormalization of quantum simulations, Phys. Rev. D **104**, 094519 (2021).

[145] D. González-Cuadra, T. V. Zache, J. Carrasco, B. Kraus, and P. Zoller, Hardware efficient quantum simulation of non-Abelian gauge theories with qudits on Rydberg platforms, Phys. Rev. Lett. **129**, 160501 (2022).
[146] M. Creutz, L. Jacobs, and C. Rebbi, Monte Carlo study of Abelian lattice gauge theories, Phys. Rev. D **20**, 1915 (1979).
[147] M. Creutz and M. Okawa, Generalized actions in $Z(p)$ lattice gauge theory, Nucl. Phys. **B220**, 149 (1983).
[148] G. Bhanot and C. Rebbi, Monte Carlo simulations of lattice models with finite subgroups of SU(3) as gauge groups, Phys. Rev. D **24**, 3319 (1981).
[149] D. Petcher and D. H. Weingarten, Monte Carlo calculations and a model of the phase structure for gauge theories on discrete subgroups of SU(2), Phys. Rev. D **22**, 2465 (1980).
[150] G. Bhanot, SU(3) lattice gauge theory in four-dimensions with a modified Wilson action, Phys. Lett. **108B**, 337 (1982).
[151] Y. Ji, H. Lamm, and S. Zhu, Gluon digitization via character expansion for quantum computers, Phys. Rev. D **107**, 114503 (2023).
[152] A. Alexandru, P. F. Bedaque, R. Brett, and H. Lamm, Spectrum of digitized QCD: Glueballs in a S(1080) gauge theory, Phys. Rev. D **105**, 114508 (2022).
[153] M. Carena, E. J. Gustafson, H. Lamm, Y.-Y. Li, and W. Liu, Gauge theory couplings on anisotropic lattices, Phys. Rev. D **106**, 114504 (2022).
[154] D. H. Weingarten and D. N. Petcher, Monte Carlo integration for lattice gauge theories with fermions, Phys. Lett. **99B**, 333 (1981).
[155] D. Weingarten, Monte Carlo evaluation of hadron masses in lattice gauge theories with fermions, Phys. Lett. **109B**, 57 (1982).
[156] J. B. Kogut, 1/N expansions and the phase diagram of discrete lattice gauge theories with matter fields, Phys. Rev. D **21**, 2316 (1980).
[157] J. Romers, Discrete gauge theories in two spatial dimensions, Ph.D. thesis, Master's thesis, Universiteit van Amsterdam, 2007.
[158] E. H. Fradkin and S. H. Shenker, Phase diagrams of lattice gauge theories with Higgs fields, Phys. Rev. D **19**, 3682 (1979).
[159] D. Harlow and H. Ooguri, Symmetries in quantum field theory and quantum gravity, Commun. Math. Phys. **383**, 1669 (2021).
[160] D. Horn, M. Weinstein, and S. Yankielowicz, Hamiltonian approach to Z(N) lattice gauge theories, Phys. Rev. D **19**, 3715 (1979).
[161] G. Clemente, A. Crippa, and K. Jansen, Strategies for the determination of the running coupling of $(2+1)$-dimensional QED with quantum computing, Phys. Rev. D **106**, 114511 (2022).
[162] M. Creutz, *Quarks, Gluons and Lattices*, Cambridge Monographs on Mathematical Physics (Cambridge University Press, Cambridge, England, 1985).
[163] M. Fromm, O. Philipsen, and C. Winterowd, Dihedral lattice gauge theories on a quantum annealer, Eur. Phys. J. Quantum Technol. **10**, 31 (2023).
[164] J. Kogut and L. Susskind, Hamiltonian formulation of Wilson's lattice gauge theories, Phys. Rev. D **11**, 395 (1975).
[165] W. Grimus and P. O. Ludl, Finite flavour groups of fermions, J. Phys. A **45**, 233001 (2012).
[166] M. A. Nielsen and I. L. Chuang, *Quantum Computation and Quantum Information: 10th Anniversary Edition* (Cambridge University Press, Cambridge, England, 2010), 10.1017/CBO9780511976667.
[167] P. Hoyer, Efficient quantum transforms, arXiv:quant-ph/9702028.
[168] R. Beals, Quantum computation of Fourier transforms over symmetric groups, in *Proceedings of the Twenty-Ninth Annual ACM Symposium on Theory of Computing* (Association for Computing Machinery, New York, United States, 1997), pp. 48–53.
[169] M. Püschel, M. Rötteler, and T. Beth, Fast quantum Fourier transforms for a class of non-Abelian groups, in *Proceedings of the International Symposium on Applied Algebra, Algebraic Algorithms, and Error-Correcting Codes* (Springer, New York, 1999), pp. 148–159.
[170] C. Moore, D. Rockmore, and A. Russell, Generic quantum Fourier transforms, ACM Trans. Algorithms **2**, 707 (2006).
[171] A. M. Childs and W. van Dam, Quantum algorithms for algebraic problems, Rev. Mod. Phys. **82**, 1 (2010).
[172] B. Eastin and E. Knill, Restrictions on transversal encoded quantum gate sets, Phys. Rev. Lett. **102**, 110502 (2009).
[173] I. L. Chuang and M. A. Nielsen, Prescription for experimental determination of the dynamics of a quantum black box, J. Mod. Opt. **44**, 2455 (1997).
[174] A. R. Calderbank and P. W. Shor, Good quantum error-correcting codes exist, Phys. Rev. A **54**, 1098 (1996).
[175] A. M. Steane, Error correcting codes in quantum theory, Phys. Rev. Lett. **77**, 793 (1996).
[176] A. Steane, Multiple-particle interference and quantum error correction, Proc. R. Soc. A **452**, 2551 (1996).
[177] A. M. Steane, Simple quantum error-correcting codes, Phys. Rev. A **54**, 4741 (1996).
[178] A. Y. Kitaev, Quantum computations: Algorithms and error correction, Russ. Math. Surv. **52**, 1191 (1997).
[179] E. Kubischta and I. Teixeira, A family of quantum codes with exotic transversal gates, Phys. Rev. Lett. **131**, 240601 (2023).
[180] A. Denys and A. Leverrier, Multimode bosonic cat codes with an easily implementable universal gate set, arXiv:2306.11621.
[181] S. P. Jain, J. T. Iosue, A. Barg, and V. V. Albert, Quantum spherical codes, arXiv:2302.11593.
[182] A. Denys and A. Leverrier, The $2T$-qutrit, a two-mode bosonic qutrit, Quantum **7**, 1032 (2023).
[183] J. M. Baker, C. Duckering, A. Hoover, and F. T. Chong, Decomposing quantum generalized Toffoli with an arbitrary number of ancilla, arXiv:1904.01671.
[184] A. Barenco, C. H. Bennett, R. Cleve, D. P. DiVincenzo, N. Margolus, P. Shor, T. Sleator, J. A. Smolin, and H. Weinfurter, Elementary gates for quantum computation, Phys. Rev. A **52**, 3457 (1995).

[185] A. Bocharov, M. Roetteler, and K. M. Svore, Efficient synthesis of universal repeat-until-success quantum circuits, Phys. Rev. Lett. **114**, 080502 (2015).

[186] P. Selinger, Efficient clifford + t approximation of single-qubit operators, Quantum Inf. Comput. **15**, 159 (2015).

[187] A. Peruzzo, J. McClean, P. Shadbolt, M.-H. Yung, X.-Q. Zhou, P. J. Love, A. Aspuru-Guzik, and J. L. O'brien, A variational eigenvalue solver on a photonic quantum processor, Nat. Commun. **5**, 4213 (2014).